Proceedings of the 2006 WSEAS/IASME International Conference on Fluid Mechanics, Miami, Florida, USA, January 18-20, 2006 (pp83-88)

Numerical Simulations of the Venturi DNA Vaccines Delivery System

YI LIU*, GEORGE COSTIGAN
Department of Engineering Science
University of Oxford
Oxford, OX2 0EP
UNITED KINGDOM
*Email: yi.liu@eng.ox.ac.uk Http: //www.eng.ox.ac.uk/pjrc

Abstract: - In this paper, we outline a unique needle-free method of delivering DNA vaccines. The underlying principle of the delivery system is harness compressed helium gas to accelerate a pre-measured dose of the DNA vaccine in micro-particle form to appropriate velocity in order to penetrate outer layer of skin to achieve an optimal immunological response. One of PowderJect developments is the Venturi system, using the venturi effect to entrain micron-sized vaccines into an established quasi-steady supersonic jet flow and accelerate them towards the target. Computational fluid dynamics is utilized to simulate the complete operation of prototype Venturi system. The key features of the gas dynamics and gas-particle interaction are presented. The overall capability of the Venturi system to deliver the particles is discussed.

Key-Words: - Numerical, Simulation, Transient, Supersonic, Nozzle, Venturi, DNA vaccines, Delivery

1 Introduction

DNA vaccines offer many advantages over more conventional vaccines, such as peptide or attenuated live pathogens [1, 2]. One advantage is that DNA vaccines are reasonably stable and can be easily prepared and harvested in large quantities. The purity of the preparation should ensure freedom from the side effects caused by contaminants of proteinaceous vaccines. Additionally, naked plasmid DNA is relatively safe and can be repeatedly administered without adverse effects. Most importantly, DNA vaccination has consistently been shown to elicit both humoral and cell-mediated immune responses.

However, various research results indicate that the route of administration and the delivery system largely affect the kinetics and magnitude of the immune response [1]. DNA vaccination efficacy may be related to the administration ability to generate professional antigen-presenting cells (APCs) expressing antigen. Intradermal immunization via gene gun can directly target antigen to professional APCs, Langerhans cells, allowing to further improve direct presentation of antigen to T cells by DNA-transfected DCs. In comparison, intramuscular immunization likely targets antigen to myocytes and the antigen encoded by DNA vaccine is eventually presented through bone marrow-derived APCs. In this setting, the number of professional APCs expressing antigen may be significantly lower compared to that generated by DNA vaccine administered intradermally via gene gun.

To enhance DNA vaccine potency, which can directly target antigen to professional APCs, Langerhans cells, we need design and optimize the specific approach of administration. To this end, we propose an alternative design of a gene gun, PowderJect system [3-5], for ballistic particle delivery. A schematic of the PowderJect delivery system, which is configured for pre-clinical use, is shown in Fig. 1.

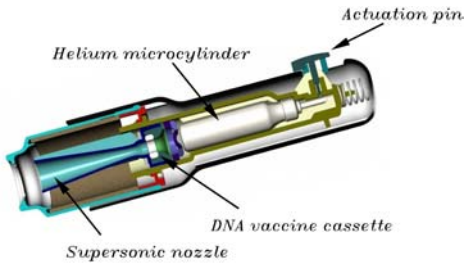

Figure 1 A schematic of the PowderJect delivery system

Its key feature is the use of energy of a shock wave to accelerate a pre-measured dose of micron DNA vaccines to appropriate momentum to impact skin or mucosal tissue. There are many advantages over a conventional needle and syringe and a liquid jet injection technology, in terms of effectiveness, cost and health risk. It is needle-free and has been shown

to be painless and applicable to a wide range of pharmaceuticals.

In this paper, a brief description of the Venturi delivery system is first given, followed by CFD methodology. The flow is then analysed by numerically solving the time-dependent Reynolds Averaged Navier-stokes (RANS) equations. The drag law is implemented to explore the particle dynamics. Comparison is made with experimental pressure measurements and Particle Image Velocimetry (PIV).

The objective of this study is to implement a numerical approach to numerically investigate the performance of the prototype Venturi device, with the primary emphasis on the over-expanded nozzle flow and the interaction between the gas and the particles.

2 The Venturi Delivery System

A unique form of PowderJect system, called the venturi powdered vaccines delivery system (Venturi), has been developed to utilize the venturi effect created in the venturi gallery to introduce powdered DNA vaccines into the delivery system [4, 5].

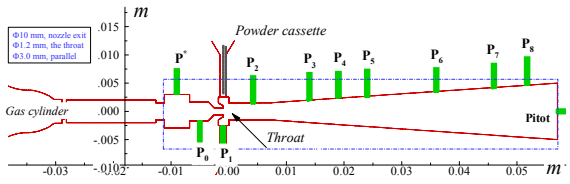

Figure 2 Configuration of the Venturi system with computational domain and experimental setup

Fig. 2 shows configuration of the Venturi device, with computational domain and experimental setup marked. The key internal components of the device are: a gas-cylinder, in which compressed Helium is stored typically at a pressure of 2-6 MPa; an externally-arranged cassette, where the powdered DNA vaccines are retained; the combination of a sonic throat, a venturi gallery and following parallel section, which is configured to form a supersonic jet and create a lower pressure cavity; a diverging conical nozzle, used to further accelerate the gas and particles to a large area, with a diameter of 10 mm at the nozzle exit.

When Helium is released from the gas-cylinder, a high pressure builds up upstream of the sonic throat, leading to the formation of a supersonic jet, which propagates down to the venturi gallery and the parallel section. A low pressure cavity is created. The area change of the diverging nozzle initiates an unsteady gas flow, as in a classical shock tube. Later, a sustained bulk flow of Helium from the cylinder is established. In the course of these processes, when a sufficient pressure difference is reached in the venturi gallery particles are entrained into the mainstream flow and accelerated towards the nozzle exit. As the gas-particle flow impinges on the skin target, gas is deflected away and vented to the atmosphere through a silencer (which is not shown here). The particles, with their relatively large inertia, maintain a high velocity and penetrate the stratum corneum into the desired tissue.

The system needs to be optimized to ensure the particles are delivered within a quasi-steady supersonic jet flow (QSSJF), and not in the starting process. This can be achieved by the choice of gas species, operating conditions and dimensions of the system geometry. The practical constraints, designed for the hand-held device, limit the device length and the duration of the QSSJF for the particles to be entrained and accelerated.

The principle of the Venturi system was initially investigated analytically and experimentally at the University of Oxford over the last few years. The over-expanded supersonic nozzle flow and resulting non-uniform particle delivery were observed. These investigations provide a useful, but incomplete indication of important flow aspects. In this paper, we will implement CFD to simulate a complete operation of prototype Venturi system.

3 Computational Methodology

Computational fluid dynamics (CFD) is utilized to simulate the gas and particle dynamics of the prototype Venturi device, including formation of supersonic jet and shock waves, interactions between supersonic jet, shock wave and the boundary layer, as well as interaction between gas phase and particle phase flow.

3.1 Mathematical models

The 2D axisymmetric Reynolds Averaged Navier-Stokes (RANS) equations are [6]

$$\frac{\partial W}{\partial t}+\frac{\partial F_i}{\partial x_i}=\frac{\partial^2 G_i}{\partial {x_i}^2}+H \qquad (1)$$

The mass fraction of each species, m_j, is predicted through the solution of a convection-diffusion equation for the j^{th} species

$$\frac{\partial}{\partial t}(\rho m_j)+\frac{\partial}{\partial x_i}(\rho m_j u_i)=-\frac{\partial}{\partial x_i}(J_{j,i})+R_j+S_j \qquad (2)$$

The equation for the particle motion, which also includes the force of gravity, is written as

$$\frac{d\vec{u}_p}{dt}=\frac{3\mu}{\rho_p D_p^2}\frac{C_D\,Re_p}{4}(\vec{u}-\vec{u}_p)+\frac{g(\rho_p-\rho)}{\rho_p} \qquad (3)$$

Given the nature of the Venturi system and the required accuracy, the standard $k-\varepsilon$ turbulence model, expression of Eq. 4, is used. It has been proven robust, economical and accurate for a wide range of turbulent flows in many industrial applications, and the shock tube based devices.

$$\rho\frac{Dk}{Dt}=\frac{\partial}{\partial x_i}\left[(\mu+\frac{\mu_t}{\sigma_k})\frac{\partial k}{\partial x_i}\right]+G_k+G_b-\rho\varepsilon-Y_M \qquad (4)$$
$$\rho\frac{D\varepsilon}{Dt}=\frac{\partial}{\partial x_i}\left[(\mu+\frac{\mu_t}{\sigma_\varepsilon})\frac{\partial \varepsilon}{\partial x_i}\right]+C_{1\varepsilon}\frac{\varepsilon}{k}(G_k+C_{3\varepsilon}G_b)-C_{2\varepsilon}\rho\frac{\varepsilon^2}{k}$$

A non-equilibrium wall function is employed to consider the effects of pressure gradient and strong non-equilibrium in the near-wall region of the Venturi device, which involves separation, possibly reattachment, and impingement.

3.2 Drag correlation

The particle trajectory solution (Eq. 3) requires the delineation of the gas flow field as well as the variation of the drag coefficient, which is related to Reynolds and Mach numbers.

It is evident that there is great discrepancy between the correlations proposed for evaluating the particle drag coefficient, C_D. These discrepancies stem from the different ranges of Reynolds and Mach number covered, gas flows, particle sizes and density ranges and the particle concentration. Regarding to our particular application, the drag correlation of Igra & Takayama [9], which cover a wider range of Reynolds number (200 to 101,000), provided the most satisfactory comparison [6-8].

$$\log_{10} C_D = 7.8231 - 5.8137\log_{10} Re + 1.4129(\log_{10} Re)^2 - 0.1146(\log_{10} Re)^3$$

3.3 Numerical approaches

The transient gas flow and its interaction with particles are modeled simultaneously and interactively. The solution of multi-species gas phase is obtained by numerically solving the RANS Eq. 1, together with turbulence model Eq. 4, and species transport Eq. 2. The particle trajectories Eq. 3, in conjunction with the drag correlation, are advanced in time with gas flow simulation. The inter-phase exchange of momentum and heat is also considered in each time step.

For the solution, Fluent [10], a commercial CFD software is chosen to numerically simulate the gas and particles flow within the prototype Venturi system. A coupled explicit solver is selected in order to capture the main features of the unsteady motion of the shock wave process. An overall second-order accuracy is satisfied both spatially and temporally to accurately predict the interaction between the oblique shock and the turbulence boundary layer.

CFD calculations with the numerical approach described here show excellent agreements with experimental measurements in shock tube based PowderJect delivery system [6-8].

4 Results and Discussion

CFD calculations with the different combination of grids, physical models and the particle drag correlations are conducted to establish grid independency, and to evaluate the drag correlations for the micro particle in the transient supersonic flow. Some representative results are presented here.

4.1 The transient gas flow

Fig. 3 shows the calculated and experimental time histories of the static pressure, with the locations marked in Fig. 2.

The calculated static pressures in Positions P_0 and P_4 before the time of 200 μs are higher than those measured and are also quite oscillatory. This is probably due to the mismatch of the inlet boundary conditions, since no measurement of the inlet total pressure or temperature is available. Rather, the pressure trace from the pressure transducer in Position P* is taken as the total pressure. This oscillation is also attributed to the assumption of a constant total temperature (taken as a room temperature). However, as indicated in Fig.3b, this discrepancy, due to the boundary condition treatment, is unnoticeable from ~ 250 μs when the supersonic jet flow is established. Furthermore, from the light obscuration experiment, it is observed for particle delivery commencing from ~ 1 ms. Hence, the implemented inlet boundary conditions are

considered acceptable as preliminary studies for the Venturi system. The pressure measurements here are averaged value over an area of 1.8 mm in diameter (the size of the pressure transducer). In general, it shows good agreement between numerical simulations and experimental measurements.

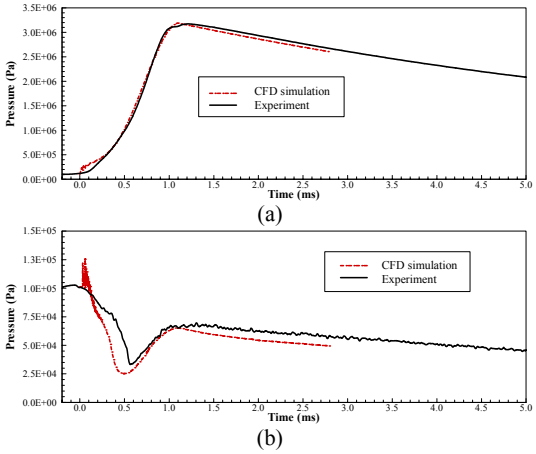

Figure 3 Comparison of simulated and experimental pressure histories, with Positions of P_0(a) and P_4(b) marked in Fig. 2

Fig. 4 shows the calculated Mach number profiles against the axial position at a range of time, illustrating the complexity of flow structures within the Venturi system.

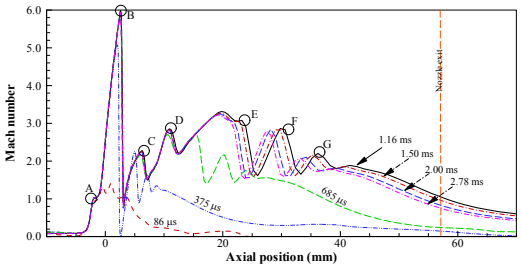

Figure 4 Computed Mach number distributions along the axis

The sonic flow is firstly reached at the throat (marked ``A" in the figure) at the time of 86 μs. Subsequently, the supersonic jet is established from ``A" to ``B". The peak Mach number is found to be about 6. As a result, a strong normal shock-like wave is generated when the jet enters the parallel section. The unsteady expansion recovers and the supersonic jet is regenerated as it flows downstream. An oblique shock is observed within the parallel section (marked ``C"). This shock cell pattern persists in the diverging nozzle, as marked ``D", ``E", ``F" and ``G". The Mach number gradually decays to 0.75 from just above 1.0 at the center of the nozzle exit plane during the time of interest (1.0-3.0 ms) for the particle delivery.

The contour plots of strain rate in the QSSJF regime (Time = 1.16 ms), together with its magnified velocity vectors near the separation zone, are displayed in Fig. 5 The strain rate, which is represented by velocity gradient along axis and radial direction, indicates the degree of flow distortion (compression/expansion waves, shocks and separations, etc.) [7]. Thus, their contour plots illustrate the flow structure characteristic. The magnified velocity vectors show a large separation bubble straight extending to the nozzle exit. It is due to a strong interaction between the oblique shock and the turbulence boundary layer, which is a dominant feature for the over-expanded supersonic nozzle flow.

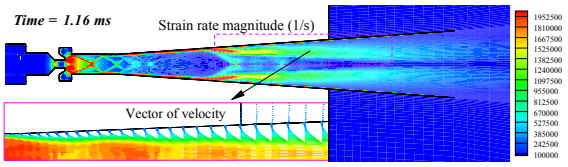

Figure 5 The computed contours of strain rate with magnified velocity vector within the QSSJF, Time=1.16~ms

It is further investigated by plotting calculated velocity profiles at 1 mm downstream of the nozzle exitplane (labeled in Fig. 4) at different time stages of interest, gathered in Fig. 6. The measured mean velocity and the standard deviation are plotted for a comparison. The experimental data were taken from the pressure measurements of Pitot probe and nearby pressure transducer P_8 at the time of 1 ms, which is considered in the QSSJF regime.

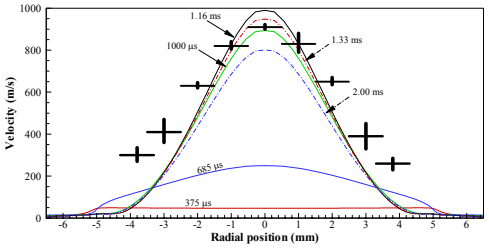

Figure 6 The computed gas velocity profiles at 1 mm downstream of the nozzle exit plane, with measured mean velocity and standard deviation marked

4.2 The particle flow

The QSSJF characteristics, generated within the prototype Venturi device, have significant effects on the particle delivery. Similar to the gas flow field, a higher particle velocity is restricted in the central core region, within the diameter of ~ 5 mm at the nozzle exit. Close to the nozzle edge, the particle velocity is quite low. We extract the calculated

particle velocity data, and plot their variations with radial position at 1 mm downstream of the nozzle exit in Fig. 7, the same position as shown in Fig. 6. The particle velocity in the free jet exhibits a wide range, ~ 400-1,000 m/s, and with few particles distributed in the outside area. This is consistent with the gas velocity distribution shown in Fig. 6.

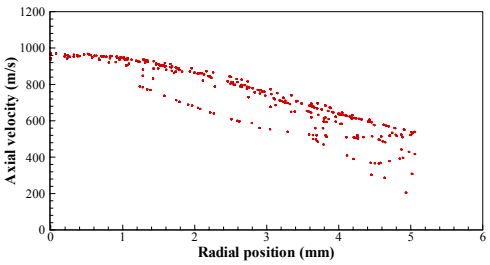

Figure 7 The computed particle velocity distributions

Fig. 8 shows a representative particle trajectory and time of the flight. The particles are accelerated rapidly within the first 5 mm due to a strong supersonic jet and a relatively large slip velocity.

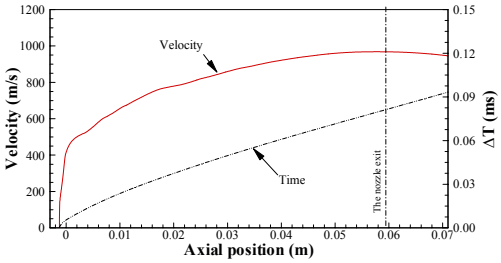

Figure 8 The computed particle trajectory and time of the flight

This pattern is confirmed by experimental penetration studies. Fig. 9 shows a typical particle `footprint' and histological image. The mean penetration depth is about 250 μm in Agar gel, with more particles evidently coring in the center area. This is consistent with the predicted gas flow field and particle simulations. The further impact studies also reveal a similar particle penetration pattern.

Figure 9 The particle footprint and histological images

5 Conclusion

In this paper, we numerically investigate transient gas and particles dynamics within a prototype Venturi system. A CFD methodology was implemented to gain new insights into the behavior of the over-expanded supersonic nozzle, used to accelerate DNA vaccines in micro-particle form to impact the human skin.

Predicted pressure histories and velocity distributions agree well with the corresponding pressure transducer and PIV measurements. Those comparisons demonstrate that the shock waves and the feature of the over-expanded supersonic nozzle flow are accurately captured with the proposed numerical approach.

The action of the gas flow accelerating the particles is calculated by implementing the drag correlation within the modeled gas flow field. It was observed gas and particle flow non-uniformities, generated by the oblique shock along with associated separation within the quasi-steady supersonic jet flow. This research is extended to new designs of the Venturi system, which can deliver particles with a narrow and more controllable velocity and spatial distribution.

Acknowledgments:
Financial supports from PowderJect Plc and Chiron Vaccines are gratefully acknowledged.

References:

[1] Trimble, C., Lin, C., *etc.*, Comparison of the CD8+ T cell responses and antitumor effects generated by DNA vaccine administered through gene gun, biojector, and syringe, Vaccine, 2003, 21(25-26), pp:4036-4042.

[2] Vassilev, V.B., Gil LHVG, Donis R.O., Microparticle-mediated RNA immunization against bovine viral diarrhea virus, Vaccine, 2001, 19(15-16), pp:2012-2019.

[3] Bellhouse, B.J., Sarphie, D.F. and Greenford, J.C., Needless Syringe Using Supersonic Gas Flow for Particle Delivery, Int. Patent WO94/24263, 1994.

[4] Liu, Y., Kendall, M.A.F., Costigan, G. and Bellhouse B.J., Prediction of Jet Flows from the Axisymmetric Supersonic Nozzle, Paper-1511, Proc. of 24th Int. Symp. on Shock Waves, Beijing, PR China, 2004.

[5] Costigan, G., Liu, Y., Brown, G.L., Carter, F.V. and Bellhouse, B.J., Evolution of the Design of the Venturi Devices for the Delivery of Dry Particles to Skin or Mucosal Tissue, Paper-2981, Proc. of 24th Int. Symp. on Shock Waves, Beijing, PR China, 2004.

[6] Liu, Y., Kendall, M.A.F., Truong, N.K. and Bellhouse, B.J., Numerical and Experimental Analysis of a High Speed Needle-free Powdered Vaccines Delivery Device, AIAA-2002-2807, Proc. of 20th AIAA Applied Aerodynamics Conference, St. Louis, USA, 2002.

[7] Liu, Y. and Kendall, M.A.F., Numerical study of a Transient Gas and Particle Flow in a High-speed Needle-free Ballistic Particulate Vaccine Delivery System, Journal of Mechanics in Medicine and Biology, 2004, 4(4), pp:559-578.

[8] Liu, Y. and Kendall, M.A.F., Numerical Simulation of Heat Transfer from a Transonic Jet Impinging on Skin for Needle-free Powdered Drug and Vaccine Delivery, Journal of Mechanical Engineering Science, Proceedings of the Institution of Mechanical Engineers Part C, 2004, 218(11), pp:1373-1383.

[9] Igra, O. and Takayama, K., Shock Tube Study of the Drag Coefficient of a Sphere in a Non-stationary Flow, Proc R. Soc. Lond. A, 1993, 442, pp:231-2467.

[10] Fluent user's guide volume, Fluent Inc. http://www.fluent.com/.